

Supplementary Materials: Photocracking Silica: Tuning the Plasmonic Photothermal Degradation of Mesoporous Silica Encapsulating Gold Nanoparticles for Cargo Release

Jonas G. Croissant ^{1,2,*} and **Tania M. Guardado-Alvarez** ³

¹ Prof. Jonas G. Croissant, Chemical and Biological Engineering, University of New Mexico, 210 University Blvd NE, Albuquerque, New Mexico 87131-0001, United States.

² Prof. Jonas G. Croissant, Center for Micro-Engineered Materials, Advanced Materials Laboratory, University of New Mexico, MSC04 2790, 1001 University Blvd SE, Suite 103, Albuquerque, New Mexico 87106, United States.

³ Dr. Tania M. Guardado-Alvarez, Department of Chemistry and Biochemistry, University of California Los Angeles, Los Angeles, CA 90095, United States.

* Correspondence: jonasc@chem.ucla.edu (J.G.C.). ORCID: 0000-0003-0489-9829

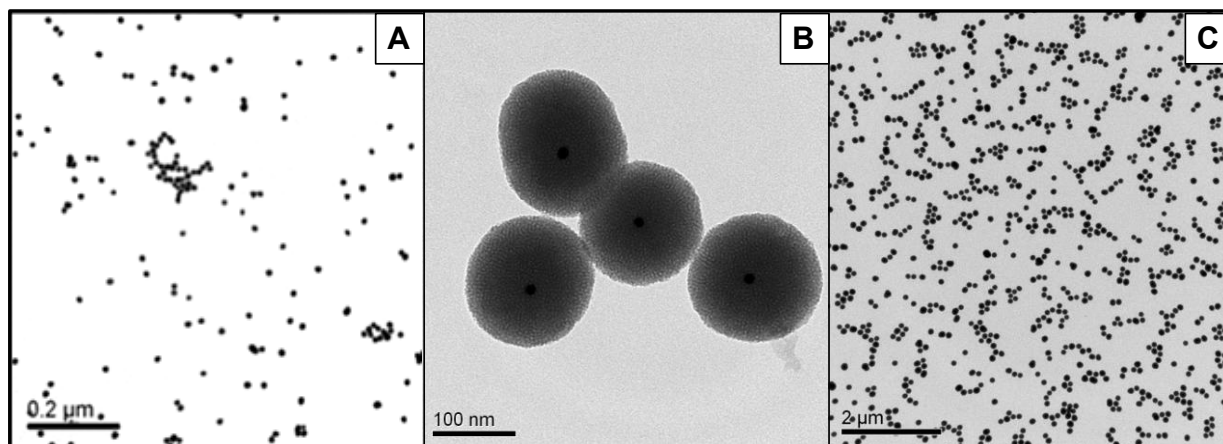


Figure S1. Transmission electron microscopy (TEM) images of monodisperse 15 nm gold nanospheres obtained by the citrate method (A) and the monodisperse Au@MSN after the core-shell synthesis (B-C).

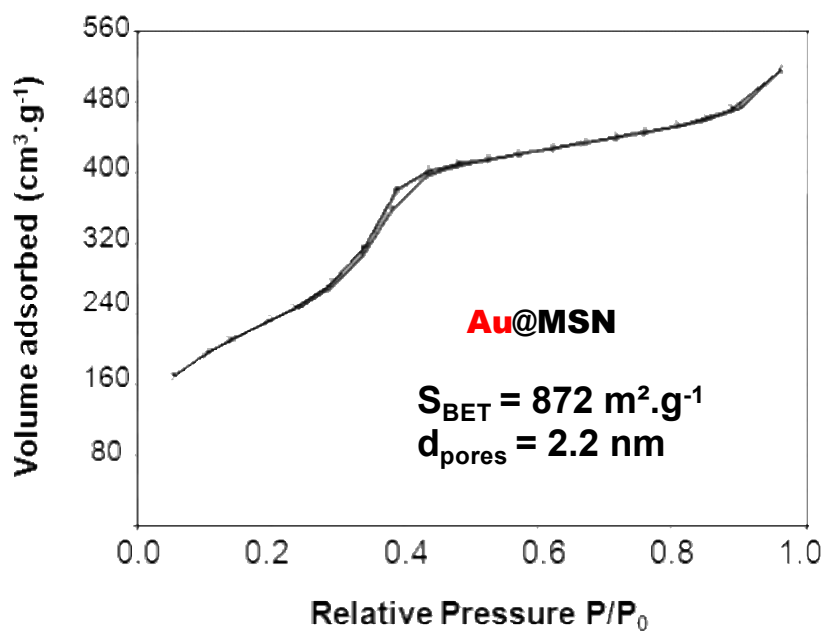


Figure S2. Nitrogen sorption isotherm of Au@MSN obtained with 15 nm monodisperse gold nanospheres (citrate method).

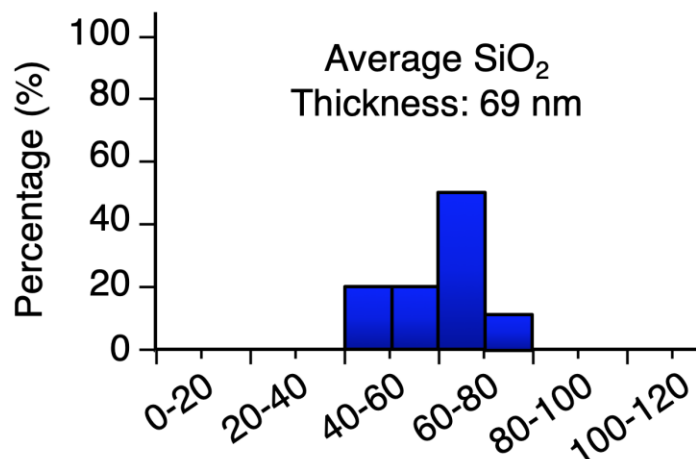


Figure S3. Histogram plotting the distribution of mesoporous silica shell thickness for Au@MSN containing monosized 15 nm-wide Au NP cores. Plotted by analyzing nanomaterials in multiple TEM images.

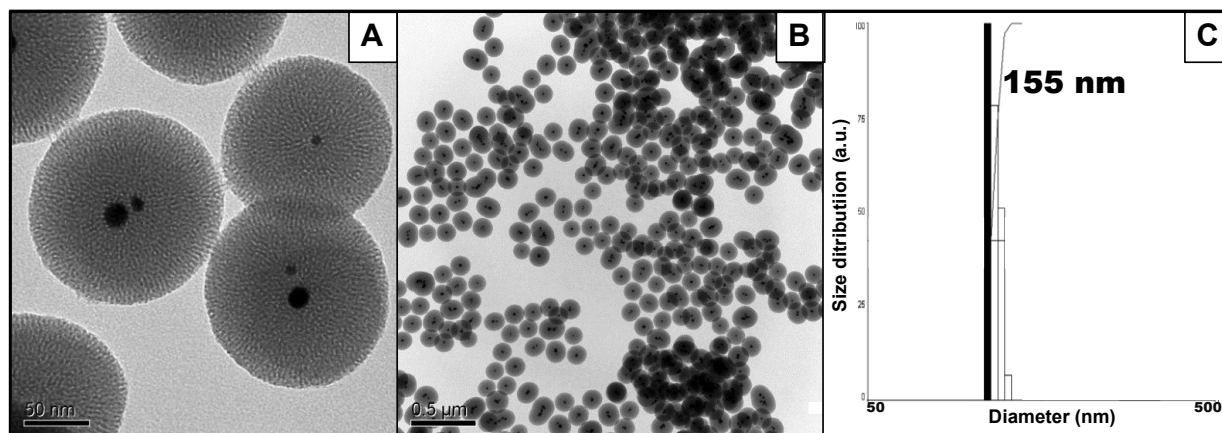


Figure S4. TEM images of monodisperse 15 nm gold nanospheres obtained by the citrate method (A) and the monodisperse Au@MSN after the core-shell synthesis (B-C).

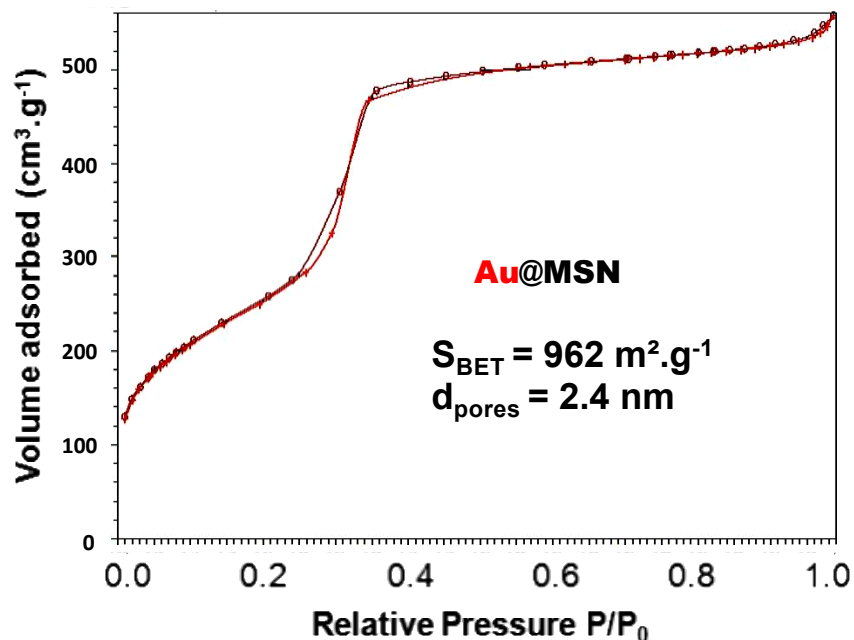


Figure S5. Nitrogen sorption isotherm of Au@MSN obtained with polydisperse gold nanospheres (in-situ method).

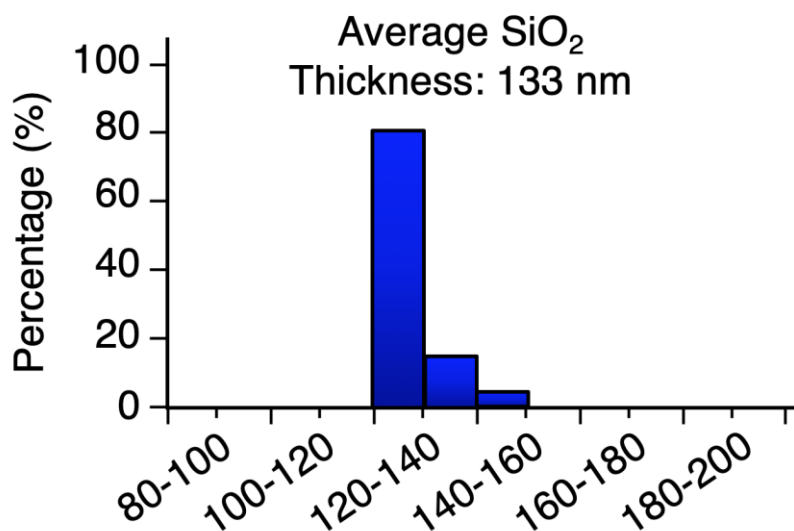


Figure S6. Histogram plotting the distribution of mesoporous silica shell thickness for Au@MSN containing polydisperse Au NP cores. Plotted by analyzing nanomaterials in multiple TEM images.

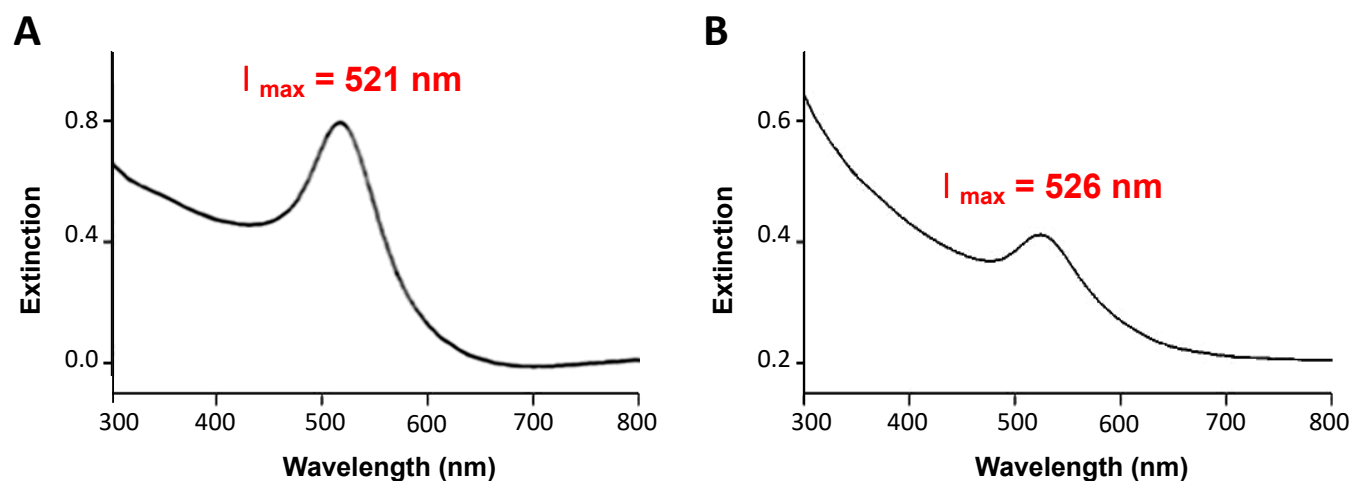


Figure S7. Extinction spectra of Au@MSN obtained with 15 nm monodisperse gold nanospheres (citrate method, A) and polydisperse gold nanospheres (in-situ method, B). Accordingly, the plasmon band of the citrate method is narrower.

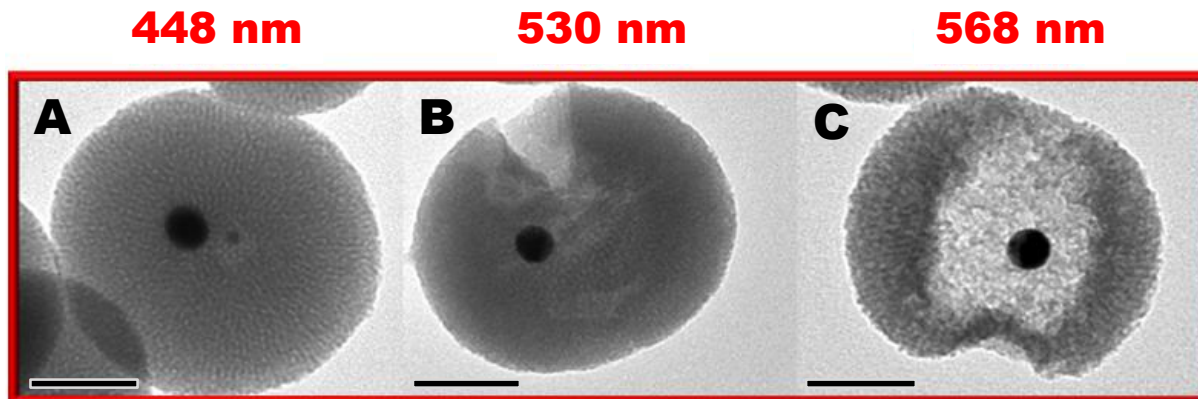


Figure S8. Wavelength dependence of the plasmonic photothermal cracking of silica demonstrated by the TEM images of irradiated Au@MSN at different wavelengths: 448 (A), 530 (B), and 568 nm (C) under 20 mW for 30 minutes.

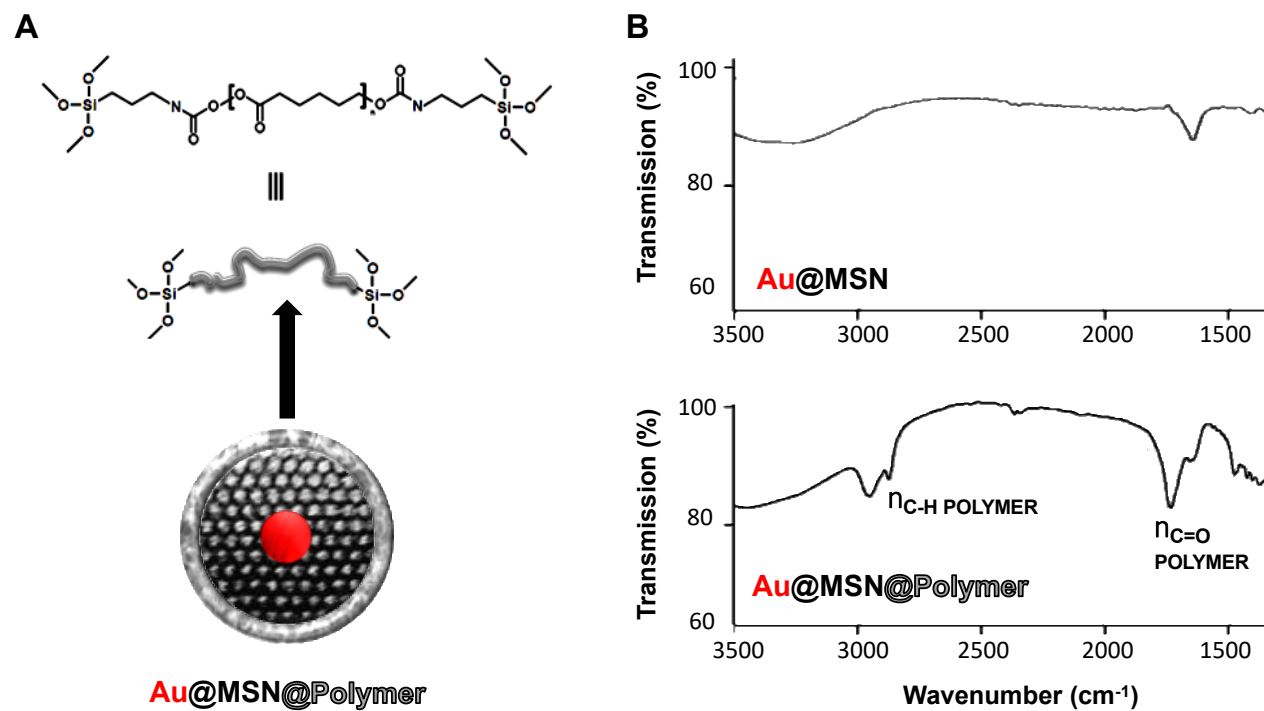


Figure S9. Representation of the Au@MSN@Polymer structure (A) and FTIR spectra confirming the polymer coating of Au@MSN.

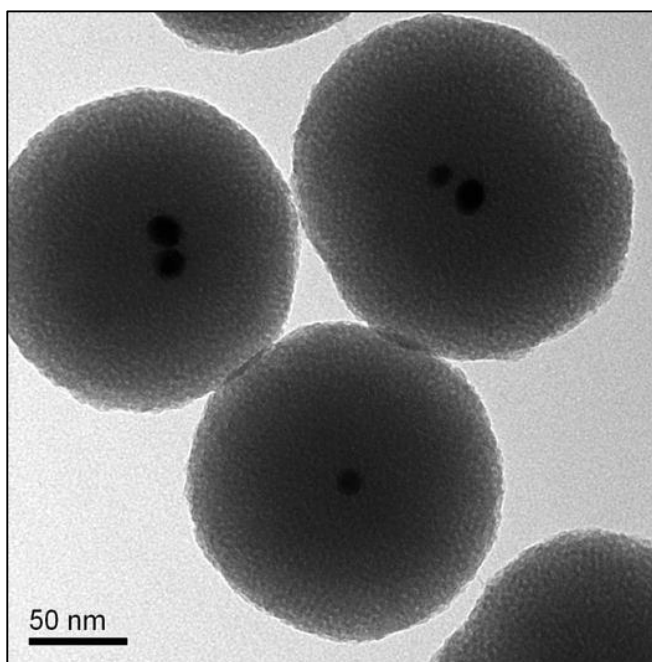


Figure S10. Representative TEM image of Au@MSN@Polymer confirming that surface coating of polycaprolactone on the particles.

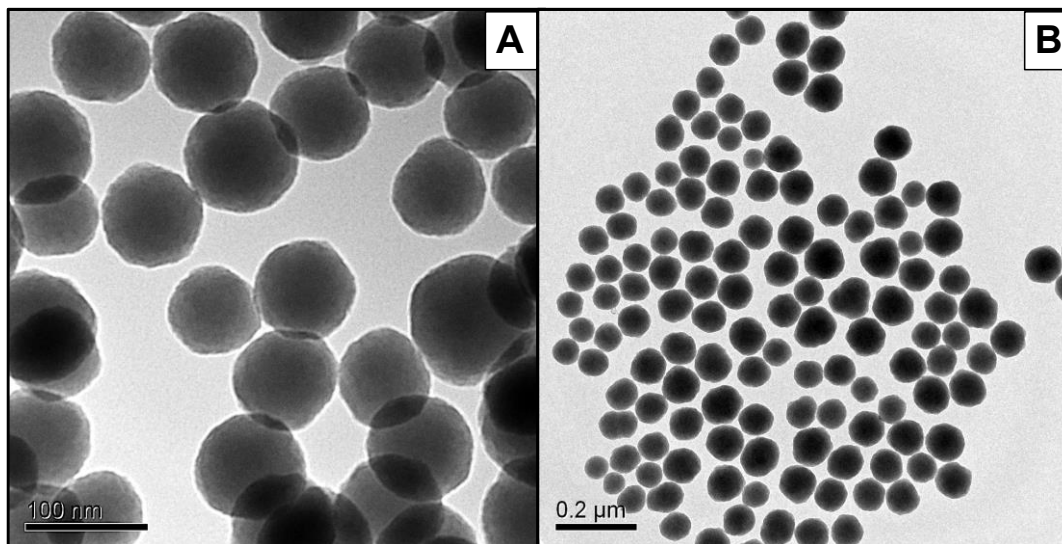


Figure S11. TEM images of solid silica nanoparticle control (non-porous equivalent used to demonstrate the loading of the cargos mainly inside the pores of MSN).

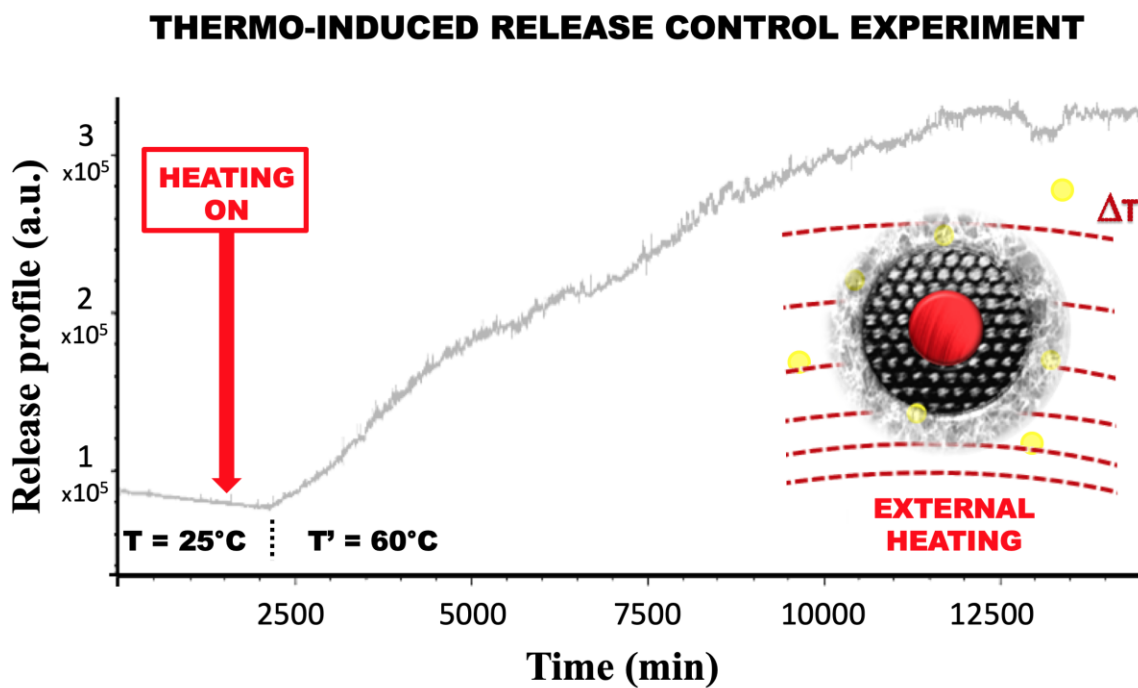


Figure S12. Thermo-induced controlled release profile of Au@MSN@ loaded with Coumarin 440. This control experiment confirms that the release of cargos is thermo-sensitive, consistent with the properties of polycaprolactone (melting point: 60 °C).

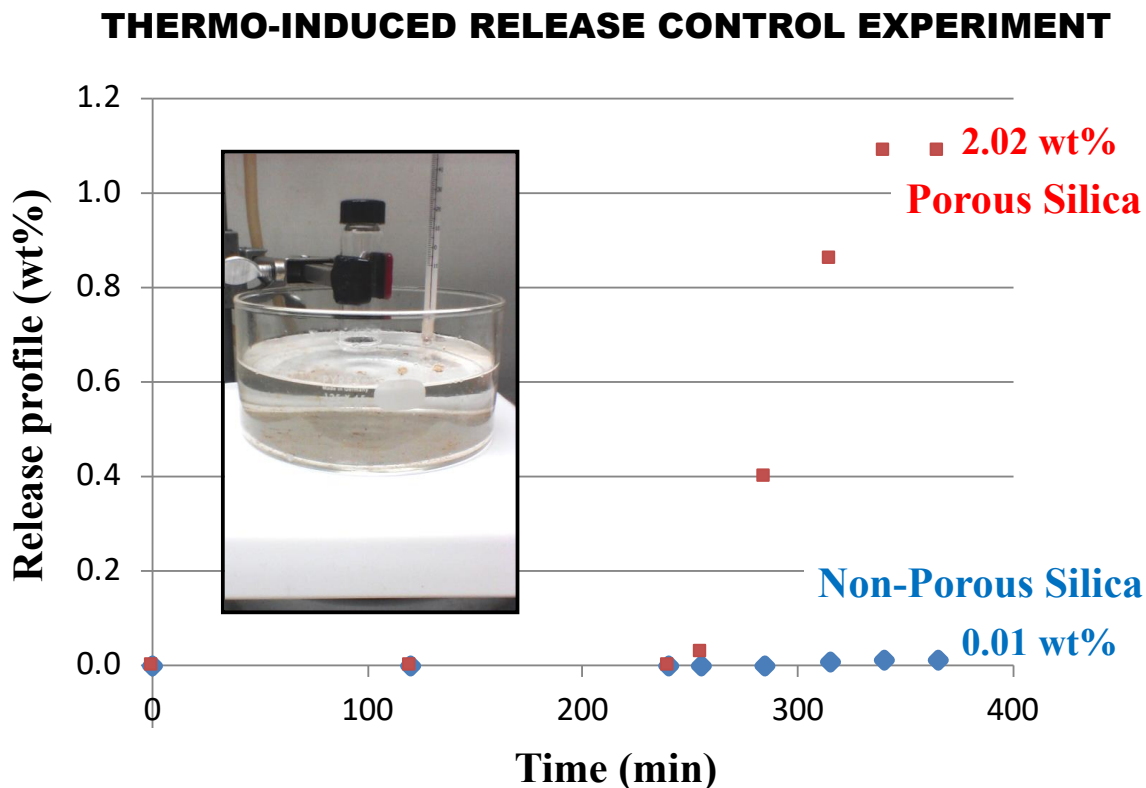


Figure S13. Thermo-induced controlled release profile of non-porous and porous silica nanoparticles coated with the polymer and loaded with rhodamine B dyes ($\Delta A_{\text{abs,max}}$ at $\lambda = 553$ nm). This control experiment shows that the loading of cargos inside polymer-coated MSN mainly occurs inside the silica pores and not inside the polycaprolactone polymer shells.